NREL subcontract XDJ-2-30630-32

Iowa State University

Quarterly Progress report for July 15-Oct 15, 2003

1. Device physics of microcrystalline Si solar cells

During this quarter, we studied the device physics of microcrystalline Si solar cells. The studies were focused on cells with a high degree of crystallinity (Raman peak ratios of ~4:1 or greater). In particular, we studied:

- Dark I(V) curves
- Open circuit voltage
- Donor and defect densities
- Changes in defect density upon compensation
- Diffusion length
- Relationship between minority carrier diffusion length and defect density

We also studied the reports in the literature related to device physics.

The following conclusions were reached:

1. Dark I(V) curves for highly crystalline materials follow standard two region I(V) curves, one dominated by junction recombination-generation current [exp (qV/2kT)], and one by neutral region diffusion limited current [exp (qV/kT)]. See Fig. 1. This conclusion may not be valid once significant amorphous fraction (~40-50%) appears in the material

2. The open circuit voltages can be deduced very well from dark I(V) curves. For example, from Fig.1, we deduce that Io, the dominant current under open-circuit conditions is 4.5E-12 A/cm^2. The voltage deduced from the short–circuit current for this cell (0.2 mA) is 0.456 V, very close to the observed voltage (0.45 V).

3. Capacitance data taken at low frequencies (100 Hz) show that the material is definitely doped, usually n type, as indicated by both Hall measurements on similar films, and QE measurements on devices. [The type of junction, (p+nn+ or p+pn+) can be deduced from QE data by studying the behavior of QE vs voltage curves for different wavelengths. When the light is shining through a thin, large gap p+ junction layer, if the QE for ~450 nm light increases significantly with reverse voltage, that says that minority carriers in the base layer, generated near the p+ layer are being collected more efficiently with increasing depletion width, i.e. the minority carriers must be electrons. Therefore, the cell must be p+pn+ type, If, on the other hand, QE for 900 nm photons increases significantly under reverse bias, but that for 450 nm does not, then we can deduce that the minority carriers are holes and the cell is p+nn+ type. We always found that , in the absence of significant compensation with B, the cells were of the p+nn+ type.] The doping densities vary between 1E17/cm^3 to 1E15/cm^3, depending upon whether the material was

compensated or not. Compensation with ppm levels of B leads to a reduction in doping density. See Fig. 2.

4. When the frequency is increased , the capacitance decreases beyond about 1 kHz (See Fig. 3) , clearly showing that there are also deep states in the material. An estimate of deep state density can be obtained using Kimerling's method [1], and the deep state density is found to be comparable to the donor density, a result in agreement with the results from the Hahn Meiner group [2]. This strong correlation between donor and deep state densities leads us to believe that possibly, the same agent (e.g. oxygen) is responsible for both types of defects. The details are in Appendix 1.

5. The device diffusion length was deduced from a measurement of QE vs. voltage. It was found to increase as the doping and defect density decreased. See Fig. 4.

6. The limitation on voltage in materials with a high degree of crystallinity comes directly from diffusion length. If the diffusion length is 1 micrometer, and the base layer is doped at a level of 1E15/cm^3, the dark current, for a hole conductivity (not drift) mobility of 10 cm^2/V-sec would be ~1.2E-10 A/cm^2. Then the voltage would be 0.49 V. Thus, to get voltages of ~0.6 V, while maintaining currents of 25-30 mA/cm^2, one must increase the diffusion length to ~10 micrometers, while keeping the thickness of the layer down to ~2-3 micrometer. A thinner layer leads to higher voltages, because the charge stored under froward bias is less than dictated by the diffusion length.

7. The decrease in fill factor vs. thickness comes from the resistance of the base layer. If the effective (including both the amorphous region near the substrate and the main microcrystalline layer) conductivity is 1E-4 S/cm, then, for a 3 micrometer thick film, the resistance is 3 ohm-cm^2. That means that one has an I.V loss of 90 mV, out of a total of 500 mV, or about 18%. Since the initial nucleating-region microcrystalline material is likely to be much more amorphous, it is not unusual to find such a total resistance and fill factor loss. Therefore, one must take care to nucleate a high degree of microcrystallinity as rapidly as possible, something that is easier to do on a metallic substrate as opposed to on tin oxide coated glass.

The major conclusions of this study are:

- One must improve the material properties to obtain diffusion lengths of the order of 10 micrometer in a material doped at ~1E16/cm^3 level.
- Keep the base layer thickness small, ~ 2-3 micrometer, to limit stored charge.
- Use conditions that lead to highly microcrystalline material as soon after growth as possible. This may mean using variable hydrogen dilution during growth, initially a very high dilution to nucleate the material, and then, less to accelerate growth.
- While one can increase the voltage by going to a less crystalline material, that will cost in terms of a decreased QE in the 800-900 nm region, which we need for a tandem cell.
- The device behavior follows the predicted results from capacitance, dark I(V) and quantum efficiency spectroscopy studies interpreted using a crystalline base layer. This fact suggests strongly that the device is limited by diffusion and not by drift.

2. Analysis of cells from MV systems

A number of microcrystalline cells from MV systems were provided for quantum efficiency, C(V) and I(V) analysis. The results have been forwarded to MV systems, and they will be reporting them in their progress report. The behavior of hole diffusion length in their cells as a function of doping is shown in Fig. 5, and follows the same pattern as in our cells.

References

1. L. C. Kimerling, Journal of Applied Physics, v 45, p 1839-1845 (1974)
2. K. Lips, P. Kanshat, W. Fuhs, Solar Energy Materials and Solar Cells, v 78, p 513-541(2003)

Vikram Dalal
PI

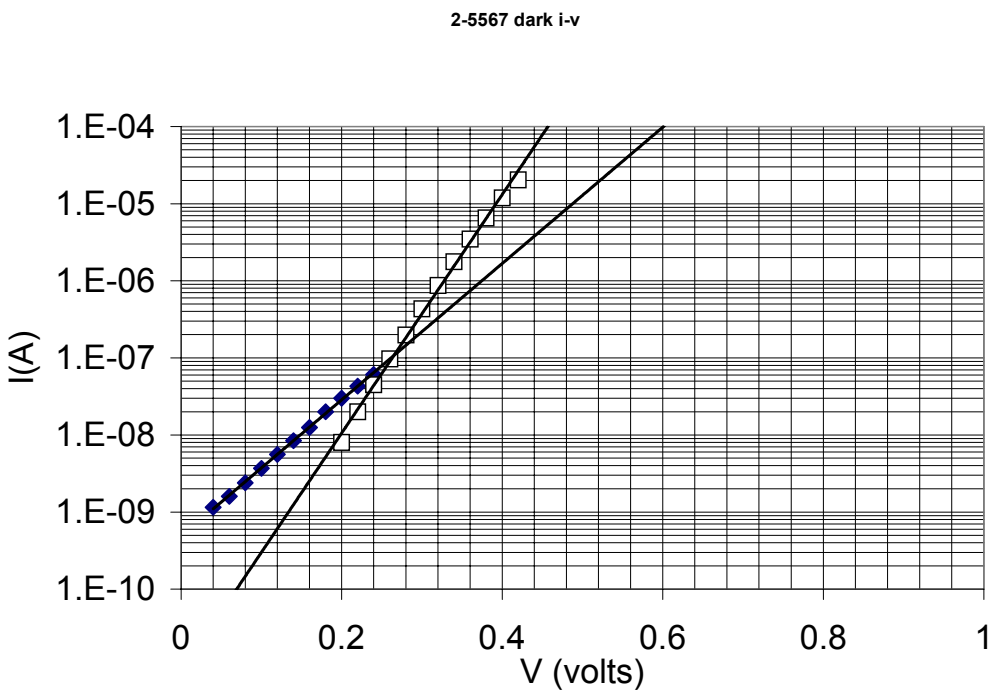

Fig. 1 Dark I(V) curve for a cell with a high degree of crystallinity

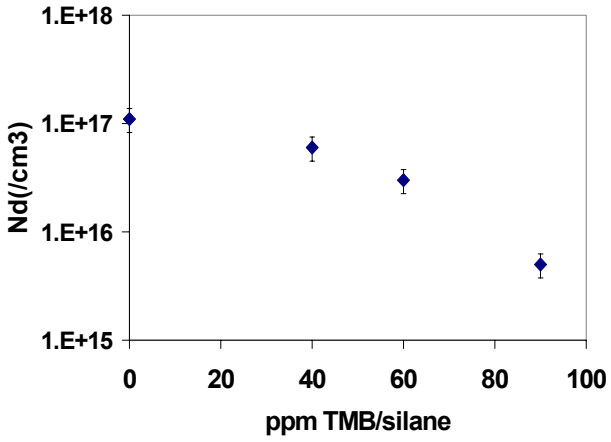

Fig. 2 Doping density vs. TMB compensation during growth

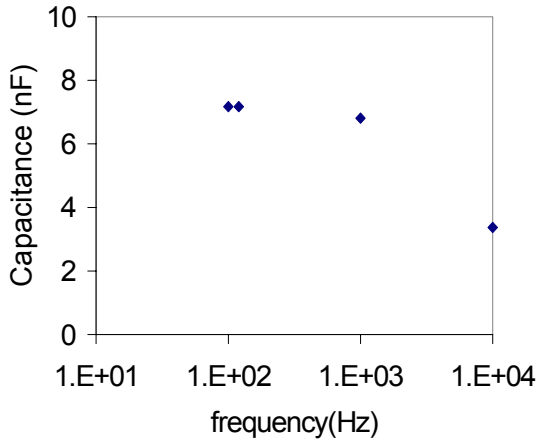

Fig. 3 Capacitance vs. frequency, clearly showing the presence of deeper states as indicated by decreasing capacitance at higher frequencies.

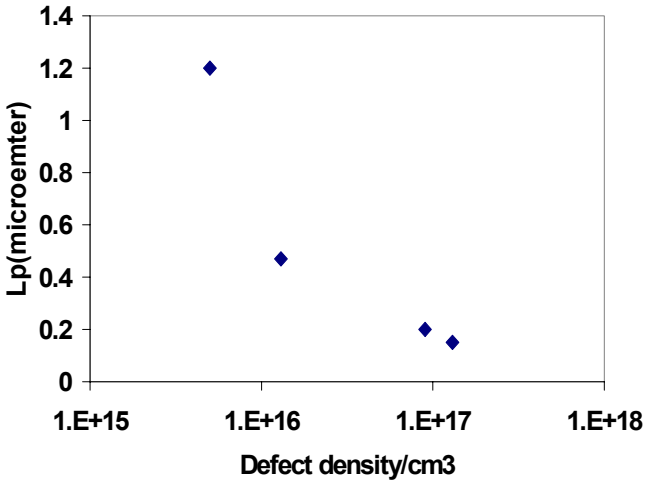

Fig. 4 Diffusion length vs. effective doping density (Iowa State samples)

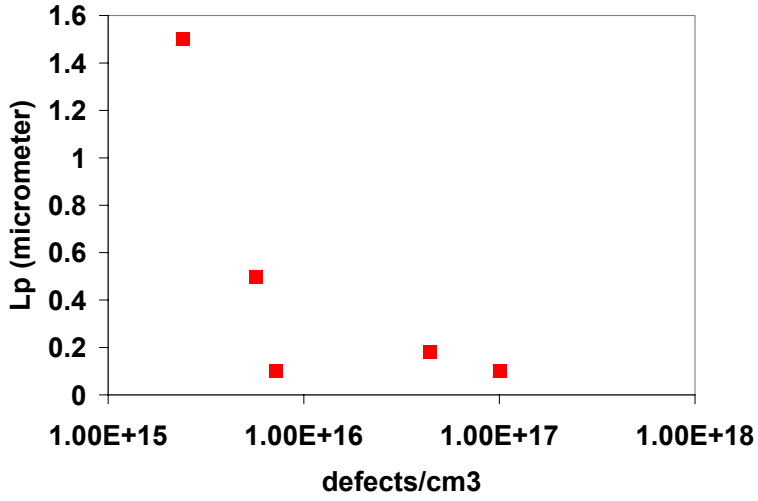

Fig. 5 Diffusion length vs. doping, MV systems samples

Appendix A

Electronic Transport in Microcrystalline Si:H and (Si,Ge):H

Vikram L. Dalal, Jianhua Zhu, Joshua Koch, Joshua Grave and M. A. Ring
Iowa State University
Dept. of Electrical and Computer Engr. and Microelectronics Research Center
Ames, Iowa, USA 50011

Abstract

We report on the electronic properties, such as defect densities and diffusion lengths of holes in microcrystalline Si:H and (Si,Ge):H materials. The microcrystalline Si:H was grown using both VHF and ECR plasma CVD discharges, whereas the microcrystalline (Si,Ge):H was grown using an ECR discharge. X-ray diffraction data indicated that the predominant orientation was <111>. All the films grown were n type. To measure material properties in devices, p^+nn^+ junctions were fabricated on steel substrates. Capacitance and quantum efficiency spectroscopy techniques were used to measure doping, defect densities and diffusion lengths of holes. It was found that the net doping concentration could be reduced by compensating with ppm levels of B. As the net doping concentration decreased, so did the total defect concentration. Diffusion lengths of holes increased as the doping decreased. Diffusion lengths of ~ 1.2 micrometer were obtained in both ECR and VHF microcrystalline Si:H. Devices with fill factors of ~70% were fabricated in microcrystalline Si:H. The diffusion lengths were lower in microcrystalline (Si,Ge):H

Introduction

Microcrystalline Si:H (μc-Si:H) is an important material for photovoltaic devices [1-6] and thin film transistor [7,8]. Most of the materials to date were grown using VHF plasma discharge (50-100 MHz frequency). There is also work using hot wire techniques [9,10] and ECR plasma techniques [11-13] to grow the material and solar cells. Solar cells approaching ~10% efficiency have been fabricated using the VHF and hot wire techniques [1,9]. Tandem cells with a-Si:H/μc-Si:H combination have resulted in efficiencies of ~ 14%. In contrast to the work on μc-Si:H, there is much less work on microcrystalline (Si,Ge):H [μc-(Si,Ge):H]. In this paper, we report on the growth and electronic properties of both material systems. The μc-Si:H was grown using both VHF and ECR deposition techniques [11-13], whereas the μc-(Si,Ge):H was grown using only the ECR growth technique[14].

Growth Techniques

The VHF plasma system used a single chamber diode geometry at 45 MHz. Typical growth rates for films and devices reported in this paper are in the range of 4 Å/s, achieved using hydrogen dilution ratios in the range of ~15:1. The pressure in the reactor was maintained at 50 mTorr. The reactor was provided with a shutter so that one could sequentially grow n, i and p layers by shielding the sample and using an in-situ plasma gettering step between layers to remove memory of the previous layer. The base vacuum in the system before deposition was $1x10^{-7}$ Torr.

The ECR growth system consisted of a single chamber, remote plasma system[11-13]. A microwave plasma with hydrogen injection was generated upstream of the sample. Silane was injected downstream from the plasma resonance zone. The pressure in the reactor had to be kept low (~ 5mT or lower) in order to achieve microcrystallinity. At higher pressures (>10 mT), the films were amorphous. This result can be explained by noting that at higher pressures, the density of the ion flux impinging on the substrate is significantly reduced [15]. This observation suggests that some degree of ion bombardment is necessary in order to grow microcrystalline films. In common with the VHF reactor, the ECR reactor was also provided with a shutter to allow sequential growth of the three layers of a cell.

Results

Results on Film Properties

A. Microcrystalline Si

X-ray diffraction spectra for a μc-Si:H sample using VHF discharge are shown in Fig.1. The most prominent peak is the <111> peak. Samples produced using ECR discharge also had the <111> peak always dominating. The grain size is ~ 15 nm. The Raman spectrum of this film is shown in Fig. 2, which clearly shows two peaks, one at 520 cm^{-1} and one at ~490 cm^{-1}. The ratio of the two peaks is 4:1.

B. Microcrystalline (Si,Ge):H

X-ray diffraction spectra for a film with 40% Ge are shown in Fig. 3. Once again, the <111> peak is dominant. The grain size is ~ 10 nm. The hydrogen dilution ratios used for producing (Si,Ge) films is found to be higher than for Si films, about 25:1. Hall measurements were

performed on some of these films. The films were found to be n type with doping of ~ 1-$2x10^{17}/cm^3$. The Hall mobilities were in the range of ~ $3cm^2/V$-sec.

Results on Diagnostic Devices

p^+-i-n^+ devices were made in the substrate geometry, with the n^+ layer being next to the stainless steel substrate. The cells consisted of a thin a-Si layer next to n+, then a microcrystalline i layer, a thin buffer layer, and a top p+ layer. In view of the fact that the undoped base layer is n type, it is more appropriate to call these cells $p^+/n/n^+$ cells. The thicknesses of the various layers were: amrophous layer ~50 nm, microcrystalline n layer, ~900 nm, buffer layer ~20 nm and p+ layer, ~30 nm. The cells were provided with a top ITO contact. The buffer layer was used between the n(i) and p^+ layers so as to improve voltage and fill factor[16].

The I(V) curve for a typical μc-Si:H cell are shown in Fig.4. The good fill factor and voltage are indications of a good quality material. No back reflector was used for these cells. These cells were used for determining material properties in devices. The I(V) curve for a similar μc-(Si,Ge):H cell is shown in Fig. 5. The voltage is lower, but the QE at 800 nm was higher compared to the case for μc-Si:H.

Results on doping and defect densities

Doping and defect densities were determined using capacitance techniques. From the work of Kimerling [17], it is known that by using a low frequency capacitance, one can estimate the total doping and defect densities by plotting the effective doping density vs. reverse voltage. At low reverse voltage, one gets an estimate of doping density alone; at higher voltages, one gets the total of (doping + deep defect) densities. In Fig. 6, we plot the $1/C^2$ vs. reverse voltage for a μc-Si:H cell. Clearly, the slope decreases (doping increases) with voltage and then saturates, as expected from Kimerling's model. From this figure, the doping density in this film was ~$5x10^{15}/cm^3$, and the defect density was comparable, also ~ $5x10^{15}/cm^3$. This near equality of doping and defect densities was seen by Lips et al previously[18]. We found that the doping (and defect) density could be reduced significantly by counter-doping the material with ppm levels of B, using Trimethylboron(TMB) as the compensating gas. See Fig. 7.

Results on Diffusion lengths of holes

Diffusion lengths of holes were measured using quantum efficiency (QE) of light with a small absorption coefficient α vs. applied voltage, in conjunction with C(V) measurements. It is known that under the conditions where $\alpha t << 1$, and $L/t << 1$, where L is the diffusion length of holes, and t is the thickness of the n base layer, QE ~ α (w+L). Therefore, by plotting QE vs. voltage, and determining the depletion width(w) vs. voltage(V) from C(V) measurements, one can determine L. w varied from ~0.1 micrometer at zero bias for heavily doped samples to ~0.5 micrometer for lightly doped samples.

In Fig. 8, we plot the QE vs. voltage curve for a VHF μc-Si:H sample with a doping density of $5x10^{15}/cm^3$. The unknown L is determined to be 1.2 micrometer. In Fig. 9, we show how L varies with doping. As the doping density reduces, L increases.

A similar QE(V) and C(V) measurement for μc-(Si,Ge):H sample yields a value for diffusion length of 0.2 micrometer.

Discussion

It is clear from the above data that materials with <111> orientation can also be of high quality. The materials are generally n type doped, with a doping density of a few $10^{16}/cm^3$. The doping density is correlated with defect density; higher the doping, higher the defect density. Perhaps this correlation is due to the presence of oxygen, an unavoidable impurity in plasma-grown films except in UHV systems. Note that doping levels did not change significantly even when back n+ layers were made in a different reactor, thus proving that the doping did not arise from previous depositions. An interesting observation is that the defect and doping densities decrease significantly upon compensation with B. Whether this is due to B-O complexes being formed, which tie up oxygen donors, or some other mechanism is not known.

From the QE and C(V) data, it is clear that the cells are behaving as classical p^+nn^+ cells, with the electric field in the n base layer being primarily restricted to the depletion region. The excellent fit of the quantum efficiency data with the model for QE vs voltage, and the capacitance results, conclusively show that for all doping levels studied, the transport is being controlled by diffusion, and not by drift.

Conclusions

In conclusion, one can fabricate good quality materials in both μc-Si:H and μc-(Si,Ge):H systems using either ECR or VHF systems. Both material systems showed a predominant <111> orientation. Diagnostic p+nn+ substrate-type devices were made in both systems on stainless steel. Capacitance measurements indicated that both the material systems had donor states and deeper defects. The defect density was correlated with the donor density; higher the donor density, higher the defect density. Both donor and defect densities were reduced significantly by compensating with B. Measurement of QE vs. voltage revealed that the data could be described well with a model which assumes that transport outside the depletion layer is by diffusion. The diffusion length for holes in μc-Si:H was estimated from such data and varied between 0.2 micrometer for heavily doped samples to 1.2 micrometer for samples with B compensation. The diffusion length in μc-(Si,Ge):H was 0.2 micrometer.

Acknowledgements

It is a pleasure to thank Kay Han, Puneet Sharma, Nanlin Wang, Durga Panda and Raegan Johnson for their technical help. The work was supported in part by NREL and in part by NSF.

References

1. Kenji Yamamoto, Masashi Yoshimi, Yuko Tawada, Susumu Fukuda, Toru Sawada, Tomomi Meguro, Hiroki Takata, Takashi Suezaki, Yohei Koi, Katsuhiko Hayashi Solar Energy Mater. And Solar Cells, 74, 449-455 (2002)

3. B. Rech, O. Kluth, T. Repmann, T. Roschek, J. Springer, J. Müller, F. Finger, H. Stiebig and H. Wagner , Solar Energy Mater. And Solar Cells, 74, 439-447(2002)

4. J. Meier, S. Dubail, S. Golay, U. Kroll, S. Faÿ, E. Vallat-Sauvain, L. Feitknecht, J. Dubail and A. Shah, Solar Energy Mater. And Solar Cells, 74, 457-467(2002)

5. O. Vetterl, F. Finger, R. Carius, P. Hapke, L. Houben, O. Kluth, A. Lambertz, A. Mück, B. Rech and H. Wagner, Solar Energy Mater. And Solar Cells, 62, 97-108(2000)

6. O. Vetterl, A. Groß, T. Jana, S. Ray, A. Lambertz, R. Carius and F. Finger, J. Non-Cryst. Solids, 299-302,p.772-777 (2002)

7. A. V. Shah, J. Meier, E. Vallat-Sauvain, N. Wyrsch, U. Kroll, C. Droz and U. Graf, Solar Energy Mater. And Solar cells, 78, Pages 469-491 (2003)

8. M. Mulato, Y. Chen, S. Wagner and A. R. Zanatta,, J.Non-Cryst. Solids,266-269,1260-1264(2000)

9. Y. Chen, K. Pangal, J. C. Sturm and S. Wagner, J.Non-Cryst. Solids, 266-269,1274-1278(2000)

10. S. Klein, F. Finger, R. Carius, B. rech, L. Houben, M. Luysberg and M. Stutzmann, Mat. Res. Soc. Symp. Proc. Vol. 715, A26.2(2002)

11. R. E. I. Schropp, P. F. A. Alkemade and J. K. Rath, Solar Energy Mater. And Solar cells, 65, 541-547 (2001)

12. V. L. Dalal and K. Erickson , Proc. Of MRS, Vol. 609(2000)

13. V. L. Dalal and K. Erickson, Proc. Of 28th. IEEE Photovolt. Spec. Conf.(2000) ,p.792-795

14. K. Erickson and V. L. Dalal, Proc. of Mater. res. Soc., 467, 409(1997)

15. K. Erickson and V. L. Dalal, J.Non-Cryst. Solids, 266, 685(2000)

16. S. Kaushal, V. L. Dalal and J. Xu, , J. Non-Cryst. Solids, 198-200, 563(1996)

17. V. L. Dalal, Jianhua Zhu and Max Noack, Proc. Of IEE(2003) To be published.

18. L. C. Kimerling, Journal of Applied Physics, v 45, p 1839-1845 (1974)

19. K. Lips, P. Kanshat, W. Fuhs, Solar Energy Materials and Solar Cells, v 78, p 513-541(2003)

Figure Captions

1. x-ray diffraction data for microcrystalline Si:H film deposited at 5 A/s. All films showed the intensity of <111> peak to be larger than that of <220> peak. The peak at 44° is due to the stainless steel substrate.

2. Raman spectrum for the film whose x-ray diffraction was shown in Fig. 1. The ratio of crystalline to amorphous peaks is ~4.

3. X-ray diffraction data for microcrystalline (Si,Ge):H film with 40% Ge deposited using ECR process. <111>, <220> and <311> peaks are clearly seen, with <111> dominating.

4. I(V) curve for microcrystalline Si:H solar cell. The current density is 14 mA/cm^2, V_{0c}=0.45 and FF=0.7. A=0.075 cm^2.

5. I(V) curve for microcrystalline (Si,Ge):H cell with 30% Ge. Voc is 0.4 V, and fill factor to 0.58, but the QE at 800 nm doubled.

6. $1/C^2$ vs. voltage curve for microcrystalline Si:H measured at 100 Hz. The value at low voltage corresponds primarily to the doping density, and the value at higher voltage corresponds to the sum of doping and defect densities, following Kimmerling's model.

7. The doping density vs. compensation level of TMB used in the gas phase.

8. QE vs voltage data. The data can be fit very well with a simple model $QE \sim \alpha (w + L)$, where L is the diffusion length, w is the depletion width, and α is the absorption coefficient. W was deduced from capacitance data such as Fig. 6.

9. Diffusion length vs, doping density for compensated samples. The doping was changed by using compensation with trimethyl Boron and then measuring diffusion lengths for each sample using the method described in Fig. 8.

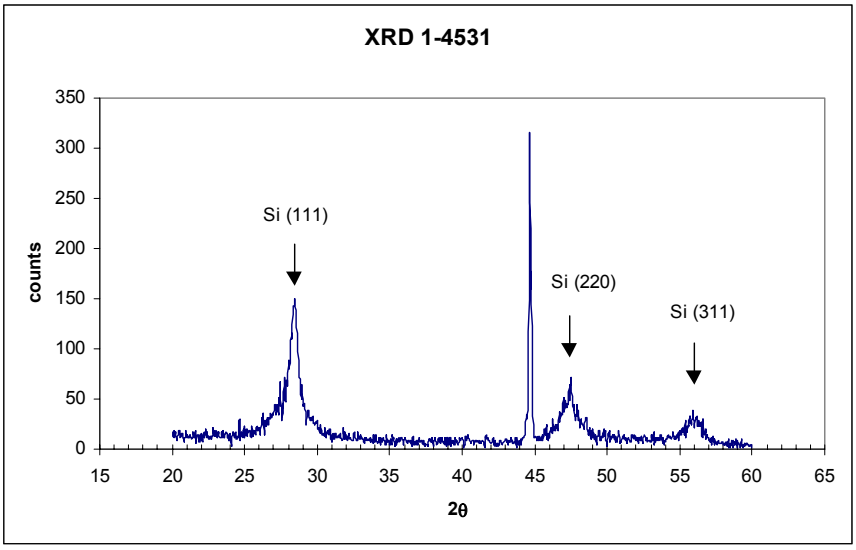
XRD 1-4531
350
300
250
200
150
100
50
0
counts
Si (111)
Si (220)
Si (311)
15
20
25
30
35
40
45
50
55
60
65
2θ

Fig. 1

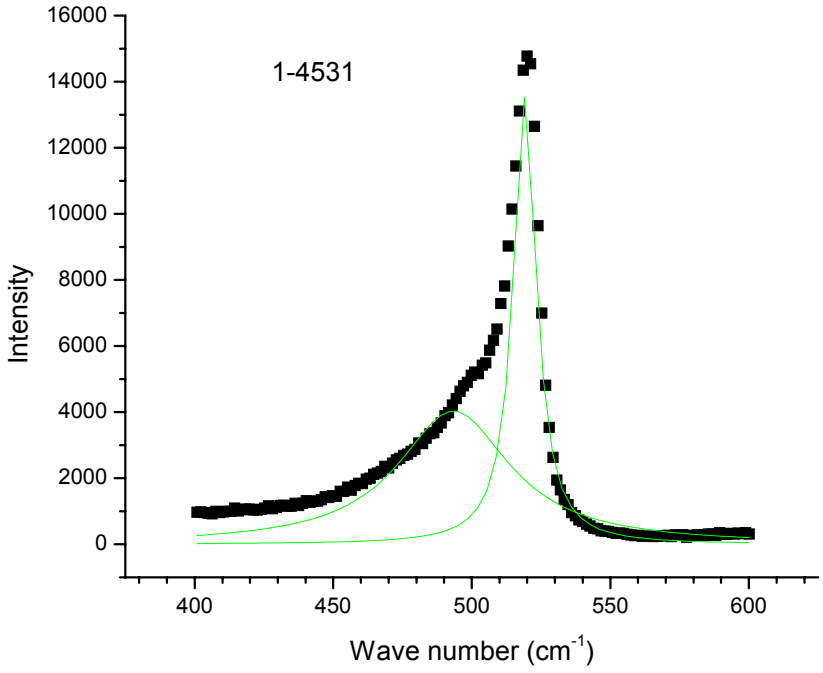
1-4531
Intensity
Wave number (cm-1)
16000
14000
12000
10000
8000
6000
4000
2000
0
400
450
500
550
600

Fig. 2

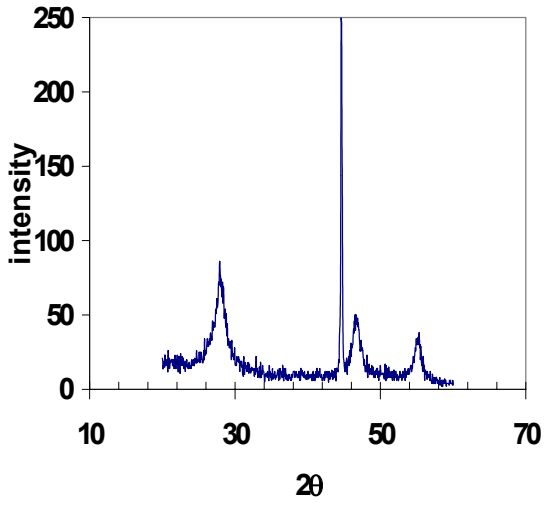

Fig. 3

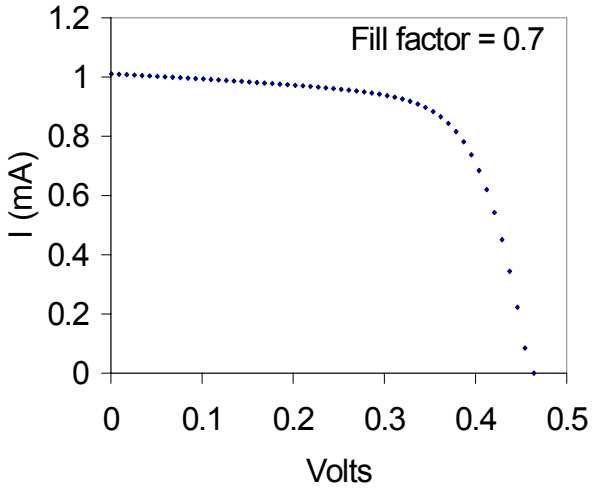

Fig. 4

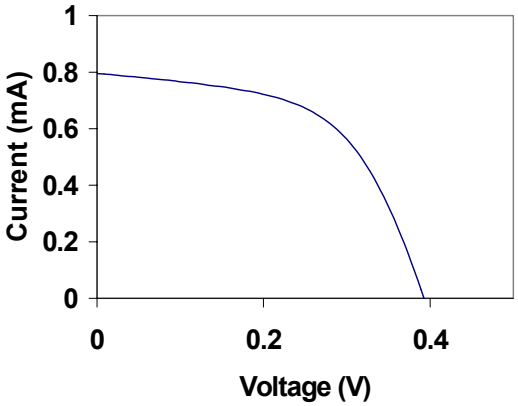

Fig. 5

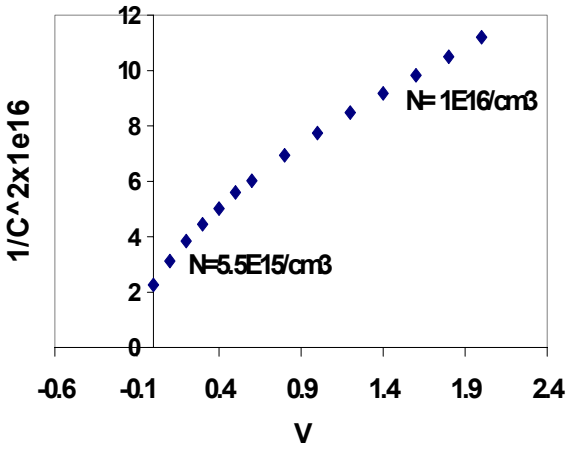

Fig. 6

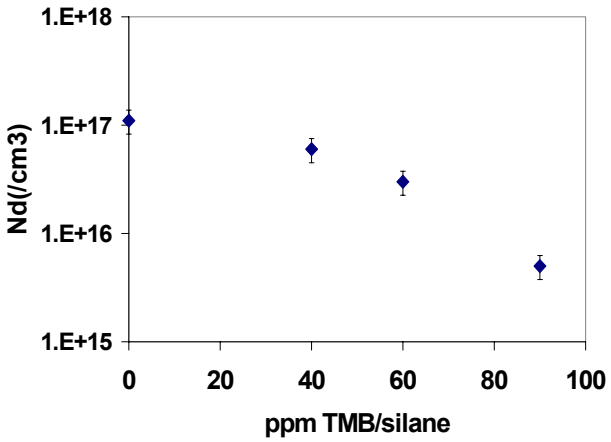

Fig. 7

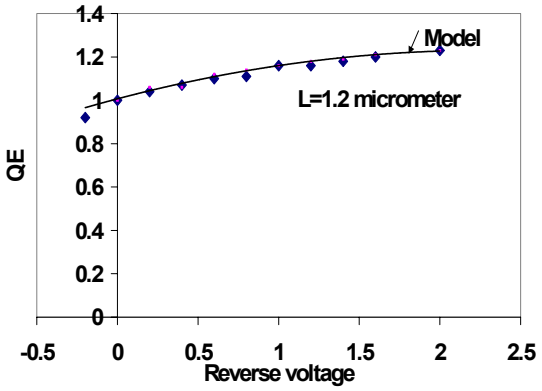
1.4
1.2
1
0.8
0.6
0.4
0.2
0
QE
-0.5
0
0.5
1
1.5
2
2.5
Reverse voltage
Model
L=1.2 micrometer

Fig. 8

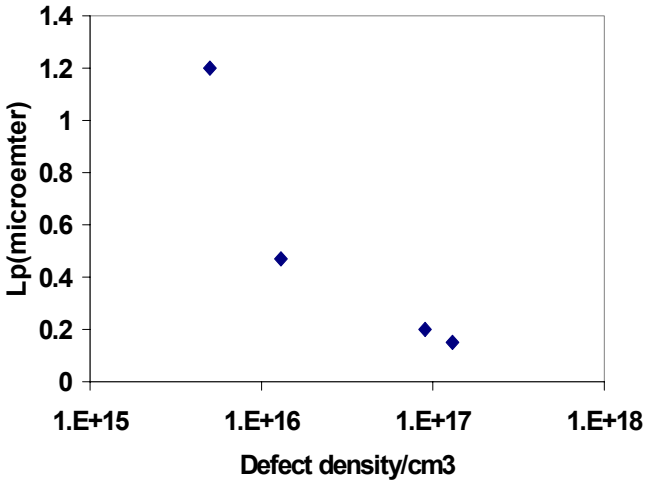
1.4
1.2
1
0.8
0.6
0.4
0.2
0
Lp(microemter)
1.E+15
1.E+16
1.E+17
1.E+18
Defect density/cm3

Fig. 9